

Issues of planning trajectory of parallel robots taking into account zones of singularity

L A Rybak¹, S Y Khalapyan², E V Gaponenko¹

¹ Belgorod State Technological University named after VG Shukhov, 46, Kostyukova St., Belgorod, 308012, Russia

² Stary Oskol Technological Institute (branch) n.a. A.A. Ugarov NUST MISiS, 42, mkr. Makarenko, Stary Oskol, 309516, Russia

E-mail: rl_bgtu@intbel.ru

Abstract. A method for determining the design characteristics of a parallel robot necessary to provide specified parameters of its working space that satisfy the controllability requirement is developed. The experimental verification of the proposed method was carried out using an approximate planar 3-RPR mechanism.

1. Introduction

Currently, the mechanisms of a parallel structure [1-5] are increasingly used in industry. In comparison with more distributed serial analogs, parallel robots have significant superiority in positioning accuracy, power and permissible load.

One of the most important sub-tasks for constructing parallel mechanisms is the determination of their design characteristics (dimensions of the fixed base, movable platform, ranges of lengths or angles of rotation of the drive links) in accordance with the necessary dimensions of the working space, i.e. a range of changes in the output coordinates.

The solution of this sub-problem is considered in the present work using a planar 3-RPR mechanism with three degrees of freedom (displacement along the x and y axes and rotation around the z axis). The mechanism consists of three kinematic chains containing one driving translational and two passive rotational kinematic pairs [6].

2. Working space

To investigate the relationship between the construction characteristics of a planar 3-RPR mechanism and the dimensions of its working space, let us use the formula for solving the inverse positional problem [7]:

$$L_i = \sqrt{(x + l_{3,i} \cos(\gamma_i + \varphi) - x_{Ai})^2 + (y + l_{3,i} \sin(\gamma_i + \varphi) - y_{Ai})^2}, (1)$$

where (x, y, φ) - output coordinates of the mechanism, γ_i - angle defining the geometry of the output link, (x_{Ai}, y_{Ai}) - coordinates of point A_i of the articulated link of the drive link to the fixed base, $l_{3,i}$ -



distance from point C_i of the articulated link of the drive to the movable platform to the point determining the position of the output link of the mechanism, and L_i - length of the i -th drive unit.

In the case of constructing a planar 3-RPR mechanism in accordance with the classical scheme of the location of attachment points A_i and C_i at the vertices of equilateral triangles, the lengths of the drive links can be determined on the basis of the following relationships:

$$L_1 = \sqrt{\left(x + \frac{r}{2}(\sin \varphi - \sqrt{3} \cos \varphi) + \frac{\sqrt{3}}{2}R\right)^2 + \left(y - \frac{r}{2}(\sqrt{3} \sin \varphi + \cos \varphi) + \frac{R}{2}\right)^2} \quad (2)$$

$$L_2 = \sqrt{\left(x + \frac{r}{2}(\sin \varphi + \sqrt{3} \cos \varphi) - \frac{\sqrt{3}}{2}R\right)^2 + \left(y + \frac{r}{2}(\sqrt{3} \sin \varphi - \cos \varphi) + \frac{R}{2}\right)^2} \quad (3)$$

$$L_3 = \sqrt{(x - r \sin \varphi)^2 + (y + r \cos \varphi - R)^2}, \quad (4)$$

where R and r - radiuses of the circles described near triangles $A_1A_2A_3$ and $C_1C_2C_3$, respectively.

The working space of the mechanism is determined by the values of R , r and the range of the lengths of the drive links and can be determined using the equations given above.

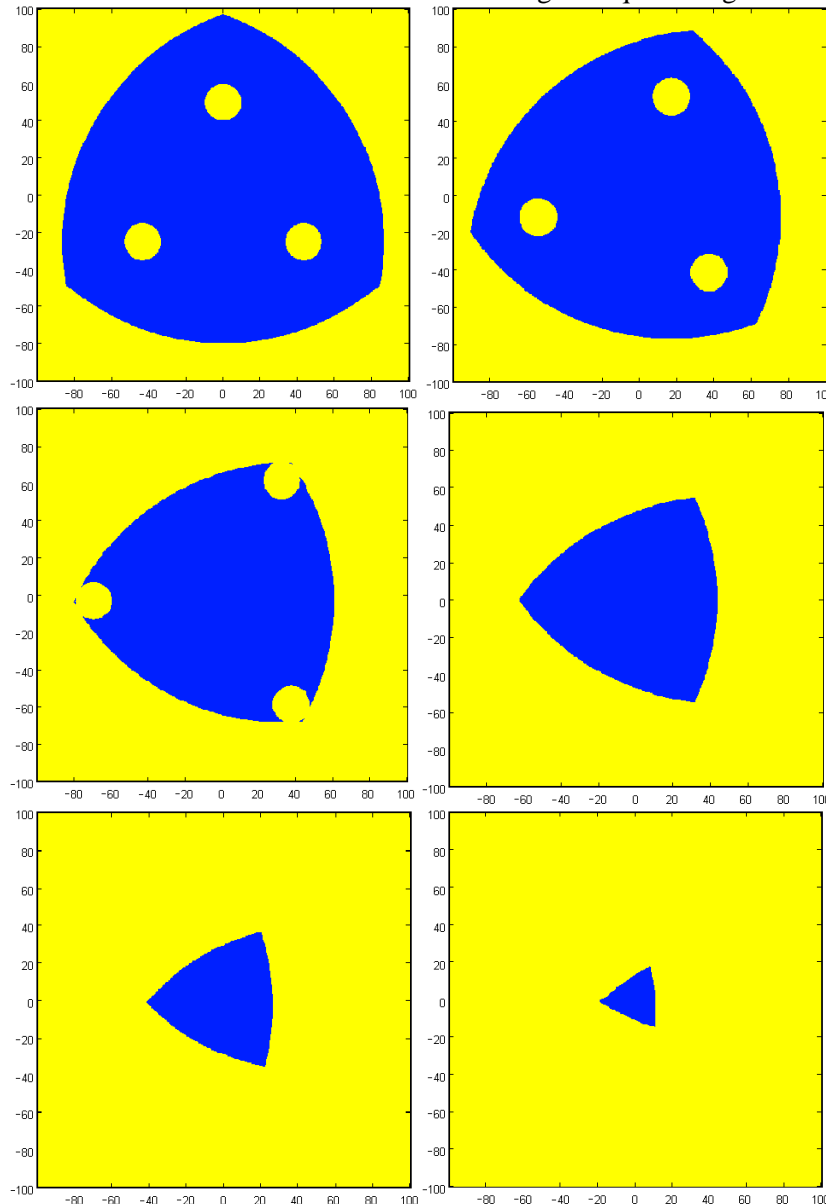


Figure 1. The range of permissible values (x, y) for $\varphi = 0^\circ, 20^\circ, 40^\circ, 60^\circ, 80^\circ, 100^\circ$.

To construct the working space of the 3-RPR mechanism, let's set its design parameters: $R = 100$ mm, $r = 50$ mm, $L_{1,2,3} \in [10 \text{ mm}, 130 \text{ mm}]$ and use the MatLAB software suite. In Figure 1 shows the areas of possible changes in the linear output coordinates of the mechanism at various angles of rotation of the movable platform (cross-section of the three-dimensional working space (x, y, φ) by planes perpendicular to the φ axis).

Figure 1 shows that with increasing angle φ , the linear size of the working area decreases. For the given construction parameters of the mechanism, the angle of rotation is 120° and is more unreachable. Obviously, in general, the smallest linear size of the working area corresponds to the largest attainable rotation angle from the range $[0^\circ, 180^\circ]$. If one sets the required linear size of the working area as a circle inscribed in it, for an angle of 180° , its diameter will be determined by the relationship (Fig.2):

$$D \leq 2(L_{\max} - R - r). \quad (5)$$

where L_{\max} - upper limit of the range of variation of the lengths of the drive links.

In this case, if the angle of 180° is unreachable (as in the case under consideration) the right-hand side of the inequality turns out to be negative.

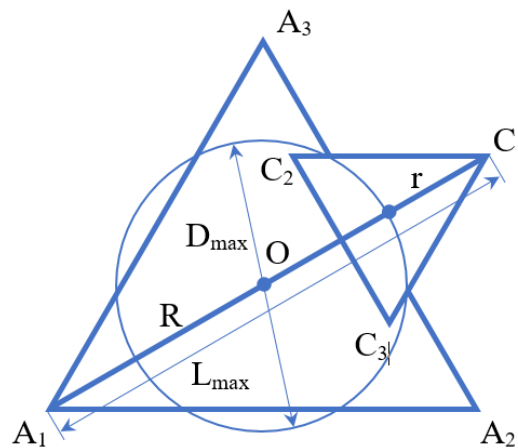


Figure 2. Dependence of D on R , r and L_{\max} .

To reduce the working space leads to the presence of "dead zones" (Figure1 displays them in the form of yellow circles). The radius of these circles is equal to L_{\min} - the lower boundary of the range of variation of the lengths of the drive links, and the distance from their centers to the center of the stationary base, as seen from Figure 3, depends on the angle of rotation of the movable platform and can be determined using the cosine theorem:

$$l = \sqrt{R^2 + r^2 - 2Rr \cos \varphi}, \quad (6)$$

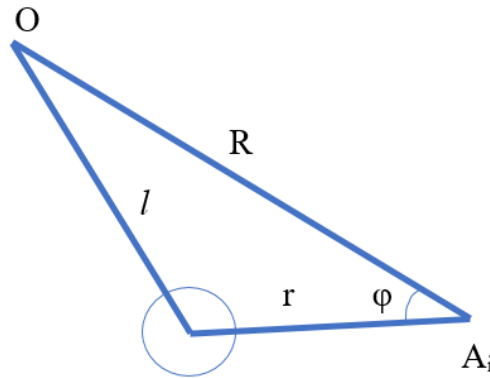


Figure 3. Dependence of l on R , r and φ .

3. Singular surface

From the working space, it is also necessary to exclude special positions of the mechanism (points of singularity). For the 3-RPR mechanism, singularities of only the second type are characteristic [2], for which the Jacobian is zero:

$$\det(J_A) = \begin{vmatrix} \frac{\partial F_1}{\partial x} & \frac{\partial F_1}{\partial y} & \frac{\partial F_1}{\partial \varphi} \\ \frac{\partial F_2}{\partial x} & \frac{\partial F_2}{\partial y} & \frac{\partial F_2}{\partial \varphi} \\ \frac{\partial F_3}{\partial x} & \frac{\partial F_3}{\partial y} & \frac{\partial F_3}{\partial \varphi} \end{vmatrix}, \quad (7)$$

where

$$\frac{\partial F_i}{\partial x} = 2x - 2x_{Ai} + 2l_{3,i} \cos(\varphi + \gamma_i), \quad (8)$$

$$\frac{\partial F_i}{\partial y} = 2y - 2y_{Ai} + 2l_{3,i} \sin(\varphi + \gamma_i), \quad (9)$$

$$\begin{aligned} \frac{\partial F_i}{\partial \varphi} = & 2l_{3,i}(y - y_{Ai} + l_{3,i} \sin(\varphi + \gamma_i)) \cos(\varphi + \gamma_i) - 2l_{3,i}(x - x_{Ai} + \\ & + l_{3,i} \cos(\varphi + \gamma_i)) \sin(\varphi + \gamma_i), \end{aligned} \quad (10)$$

that in the case under consideration means:

$$\frac{\partial F_1}{\partial x} = 2x + r(\sin \varphi - \sqrt{3} \cos \varphi) + R\sqrt{3}, \quad (11)$$

$$\frac{\partial F_2}{\partial x} = 2x + r(\sin \varphi + \sqrt{3} \cos \varphi) - R\sqrt{3}, \quad (12)$$

$$\frac{\partial F_3}{\partial x} = 2x - 2r \sin \varphi, \quad (13)$$

$$\frac{\partial F_1}{\partial y} = 2y - r(\sqrt{3} \sin \varphi + \cos \varphi) + R, \quad (14)$$

$$\frac{\partial F_2}{\partial y} = 2y + r(\sqrt{3} \sin \varphi - \cos \varphi) + R, \quad (15)$$

$$\frac{\partial F_3}{\partial y} = 2y + 2r \cos \varphi - 2R, \quad (16)$$

$$\frac{\partial F_1}{\partial \varphi} = r(x(\sqrt{3} \sin \varphi + \cos \varphi) + y(\sin \varphi - \sqrt{3} \cos \varphi) + 2R \sin \varphi), \quad (17)$$

$$\frac{\partial F_2}{\partial \varphi} = r(x(-\sqrt{3} \sin \varphi + \cos \varphi) + y(\sin \varphi + \sqrt{3} \cos \varphi) + 2R \sin \varphi), \quad (18)$$

$$\frac{\partial F_3}{\partial \varphi} = 2r((R - y) \sin \varphi - x \cos \varphi). \quad (19)$$

Substitution gives the following result:

$$\det(J_A) = 12\sqrt{3}Rr \sin \varphi (R^2 - 2Rr \cos \varphi + r^2 - x^2 - y^2). \quad (20)$$

Thus, the Jacobian is reset when one of the two conditions is fulfilled:

$$\begin{cases} \sin \varphi = 0, \\ x^2 + y^2 = R^2 - 2Rr \cos \varphi + r^2. \end{cases} \quad (21)$$

The first condition is satisfied for $\varphi = \pi n$, $\forall n \in \mathbb{Z}$. This, in particular, means that in Figure 1 the entire plane corresponding to $\varphi = 0^\circ$ is singular, which explains Figure 4, from which it can be seen that with zero rotation of the movable platform, the three straight lines A_1C_1 , A_2C_2 and A_3C_3 intersect at one point - the

center of homothety, which moves points A_i to points C_i . A similar situation is formed for $\varphi = \pm 180^\circ$, but in this case segments A_1C_1 , A_2C_2 and A_3C_3 themselves intersect, which makes such turn technically unrealizable.

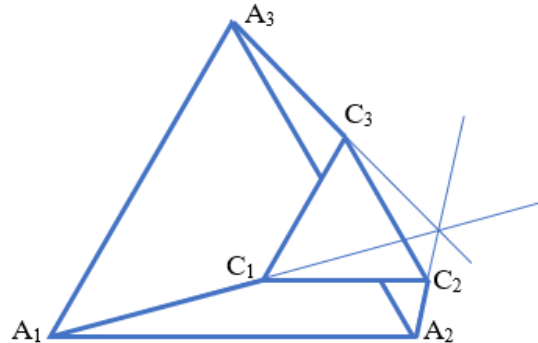


Figure 4. The singular plane at $\varphi = 0^\circ$.

Therefore, the range of permissible values of the angle of rotation of the mobile platform is determined by the inequality:

$$0^\circ < \varphi < 180^\circ \text{ (or } -180^\circ < \varphi < 0^\circ \text{)}. \quad (22)$$

The second condition of equality to zero of the Jacobian according to (21) is the equation of the circle with respect to the coordinates x and y . The radius of this circle depends on the angle of rotation of the movable platform and coincides with the value of l , determined by the formula (6).

Consequently, the singular circle passes through the centers of circles excluded from the working region in connection with the inequality of the lower boundary of the range of variation of the lengths of the drive links. This conclusion is confirmed by Figure 5, in which on the section of the working space, corresponding to the different angles of rotation of mobile platforms, applied field singularity (dark blue circle), and the Jacobian constant sign ($\det(J_A) > 0$ in the red and green areas, $\det(J_A) < 0$ - in blue and yellow).

4. Controllability

It can be seen from formula (20) that the Jacobian is a continuous function of x , y , and φ . Therefore, if two states of the mechanism are characterized by different signs of the Jacobian, the transition from one state to another without crossing the singular surface of rotation is impossible. This circumstance further restricts the working space of the mechanism.

Thus, the requirement of controllability forces us to abandon a part of the working space and to prefer (in view of the much larger size and the absence of internal "deadzones") the region inside the singular surface (shown in red in Figure 5).

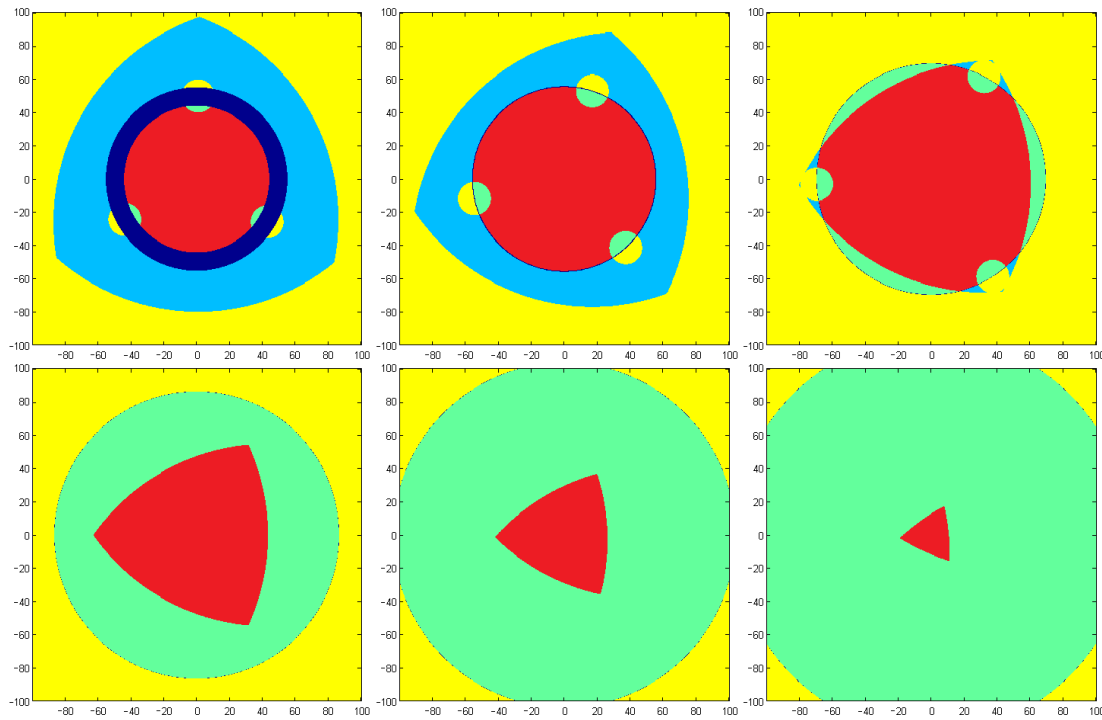


Figure 5. The range of permissible values (x, y) for $\varphi = 1^\circ, 20^\circ, 40^\circ, 60^\circ, 80^\circ, 100^\circ$, taking into account the controllability of the mechanism.

The infimum of radius l of the singular circle corresponds to $\varphi \rightarrow 0$:

$$\inf_{\varphi \in (0, \pi)} l = \lim_{\varphi \rightarrow 0+} l = \sqrt{R^2 + r^2 - 2Rr} = |R - r|. \quad (23)$$

If, as was suggested above, to set the required linear dimension of the working area in the form of a circle inscribed into it, then, taking into account the size of the "dead zones", its diameter will be determined by the relation:

$$D \leq 2(|R - r| - L_{\min}). \quad (24)$$

Combining conditions (5) and (24), let us obtain a system of inequalities that determine the diameter of the base of the cylinder, which can be inscribed in the working region of the mechanism provided that its height, i.e. the length of the range of the required change in the angle of rotation of the movable platform, is selected in accordance with condition (23).

Now, in order to determine the construction characteristics of the planar 3-RPR mechanism necessary to provide the specified parameters of its working space that satisfy the manageability requirement, it is sufficient to specify the dimensions of the fixed base and the mobile platform:

$$\begin{cases} L_{\max} \geq R + r + D/2, \\ L_{\min} \leq |R - r| - D/2; \end{cases} \quad (25)$$

or the range of variation of the lengths of the drive links:

$$\begin{cases} r \leq (L_{\max} - L_{\min} - D)/2, \\ L_{\min} + r + D/2 \leq R \leq L_{\max} - r - D/2; \end{cases} \quad (26)$$

in the case where $R \geq r$ is assumed.

5. Verification of the methodology

Let us choose, for example, the contraction characteristics that provide for the angles of rotation from 1° to 179° the displacement of the center of the movable platform within a circle with a center at the origin and with a diameter of 120 mm. Let R be 100 mm, $r = 25$ mm. According to (25):

$$\begin{cases} L_{\max} \geq 100 + 25 + 120/2 = 185, \\ L_{\min} \leq |100 - 25| - 120/2 = 15. \end{cases} \quad (27)$$

Let us take (with some margin) $L_{1,2,3} \in [10 \text{ mm}, 190 \text{ mm}]$ and check the availability (belonging to the workspace), and also the Jacobian's positivity for the points of the cylinder formed by the inequalities:

$$\begin{cases} 1^\circ \leq \varphi \leq 179^\circ, \\ x^2 + y^2 \leq 120^2. \end{cases} \quad (28)$$

The computational experiment shows that the given range of variation of the output parameters of the mechanism is located inside the selected area of its working space with a constant sign Jacobian. This means that from any state within a given range, the mechanism by changing the lengths of the drive links can be transferred to any other state from this range.

As an illustration, Figure 6 shows the areas of possible changes in the linear output coordinates (x, y) of the mechanism, taking into account its controllability at $\varphi = 1^\circ$ and 179° , and Figure 7 - coordinates (φ, y) at $x = 0$ (cross-section of the working space perpendicular to the x axis). It can be seen from the figures that the shaded figures - the base of the cylinder and its longitudinal cross-section - are completely placed in the red area.

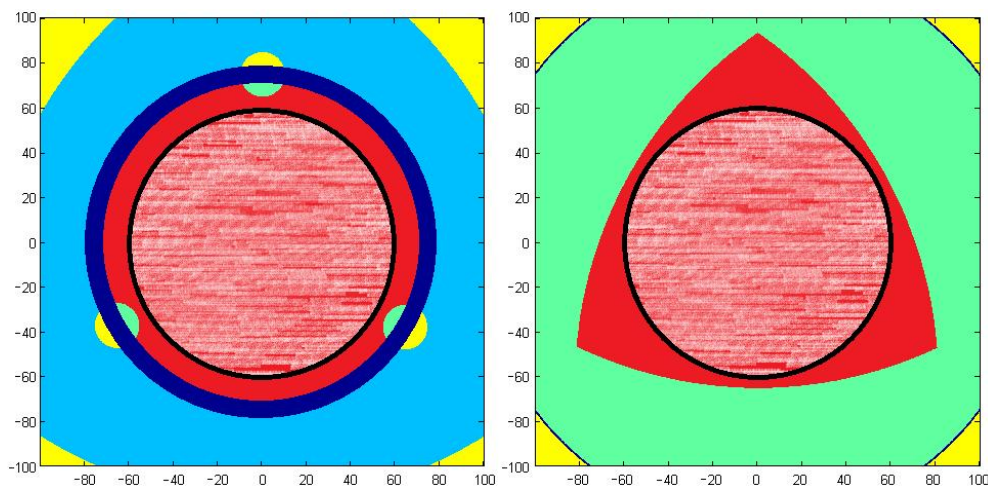


Figure 6. The region of permissible values (x, y) for the mechanism with the selected parameters for $\varphi = 1^\circ$ and 179° , taking into account the controllability.

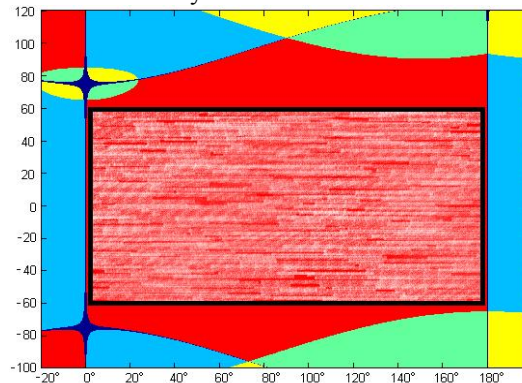


Figure 7. The range of permissible values (φ, y) for the mechanism with the selected parameters at $x = 0$ with allowance for controllability.

6. Conclusion

Thus, the method of determining the construction characteristics of a parallel robot, which is necessary to provide specified parameters of its working space that satisfy the controllability requirement, finds an experimental confirmation.

7. Acknowledgments

This work was supported by the Russian Science Foundation, agreement number 16-19- 00148, using equipment of High Technology Center at BSTU named after V.G. Shoukhov.

References

- [1] Khalapyan S Y, Rybak L A, Glushchenko A I, Mamaev Y A 2016 *International Journal of Pharmacy & Technology* **8(4)** 25085-25095
- [2] Merlet J-P 2006 *Parallel Robots Second Editio*). (Springer)
- [3] Kong X, Gosselin C 2007 *Type Synthesis of Parallel Mechanisms*. Springer
- [4] Rybak L A, Malyshev D, Chichvarin 2016 *Advances in Mechanism Design II. Proceedings of the XII International Conference on the Teory of Machines and Mechanisms* (Liberec, Czech)
- [5] Glazunov V A, Koliskor A S, Krainev A F 1991 *Spatial mechanisms of parallel structure*. (Moscow: Nauka)
- [6] Erastova K G, Laryushkin P A 2016 *Engineering Bulletin. Electronic scientific and technical journal of Bauman MSTU. Bauman* **7** 1-7
- [7] Laryushkin P A, Epanchintseva D S 2015 *Engineering Bulletin. Electronic scientific and technical journal of Bauman MSTU* **9** 12-21